Separate effects of surface roughness, wettability, and porosity on the boiling critical heat flux

Separate Effects of Surface Roughness, Wettability and Porosity on the Boiling Critical Heat Flux

Harry O'Hanley[1], Carolyn Coyle[1], Jacopo Buongiorno[1,a), Tom McKrell[1], Lin-Wen Hu[2], Michael Rubner[3], and Robert Cohen[4]

[1] Department of Nuclear Science and Engineering, Massachusetts Institute of Technology, Cambridge, Massachusetts 02139, USA

[2] Nuclear Reactor Laboratory, Massachusetts Institute of Technology, Cambridge, Massachusetts 02139, USA

[3] Department of Materials Science and Engineering, Massachusetts Institute of Technology, Cambridge, Massachusetts 02139, USA

[4] Department of Chemical Engineering, Massachusetts Institute of Technology, Cambridge, Massachusetts 02139, USA

Abstract

The separate effects of surface wettability, porosity, and roughness on the critical heat flux (CHF) of water were examined using engineered surfaces. Values explored were 0, 5, 10 and 15 μm for R_z (roughness), <5°, ~75° and >110° for static contact angle (wettability), and 0 and 50% for pore volume fraction. The porous hydrophilic surface enhanced CHF by 50-60%, while the porous hydrophobic surface resulted in a *reduction* of CHF by 97%. Wettability had little effect on the smooth non-porous surface CHF. Surface roughness (R_a, R_q, R_z) had no effect on CHF within the limit of this database.

Nucleate boiling is a common and effective energy transfer mechanism, bounded at high heat fluxes by the so-called critical heat flux (CHF) limit. CHF occurs when a continuous vapor film develops on the boiling surface, which results in a sudden, large reduction in the heat transfer coefficient. In applications where the heat flux is fixed, e.g., nuclear fuel rods and electronics cooling, the occurrence of CHF causes a rapid escalation of the surface temperature which can damage the surface itself [1]. Therefore accurate knowledge and in general enhancement of the CHF value are important to the design of systems that use nucleate boiling heat transfer. Optimization of CHF has largely been a trial-and-error process, primarily due to the complex nature of the CHF and boiling phenomena. Earlier models of CHF [2,3], still widely reported in heat transfer textbooks and handbooks, assumed that CHF is a hydrodynamic instability

---

a) Author to whom correspondence should be addressed. Electronic mail: jacopo@mit.edu

phenomenon and thus ignored the effects of the boiling surface characteristics altogether. However, the experimental evidence suggesting the importance of surface effects on CHF is clear. For example, in the experiments of Forrest *et al.* [4] and Kim *et al.* [5], comparative CHF tests for a bare boiling surface and one with a thin porous layer of nanoparticles were conducted with the same fluid and identical procedure: the value of the CHF for the surface with the porous layer was ~100% and ~200% higher than for the clean surface, respectively. Other researchers have proposed that *wettability*, *roughness* and *porosity* are the key surface parameters that affect CHF [6-14].

Wettability is the affinity of a surface to the fluid of interest, and is typically described by the contact angle, β, at the triple contact line between vapor, liquid, and the solid surface. Contact angle on a smooth surface is only a function of the fluid and surface materials. If the surface is not smooth, the contact angle changes: Wenzel [15] defines a roughness factor, r, as the ratio of the actual liquid/solid contact area to the projected area under the liquid. Then Young's equation becomes:

$$\cos \beta^* = \frac{\gamma_{SV} - \gamma_{SL}}{\sigma} r = r \cos \beta \tag{1}$$

where β^* is the apparent contact angle, $\gamma_{SV} - \gamma_{SL}$ is the adhesion tension and σ is the liquid surface tension. Eq. 1 suggests that a large value of r has the effect of making intrinsically hydrophilic surfaces ($\beta < 90°$) even more hydrophilic ($\beta^* < \beta$) and hydrophobic surfaces ($\beta > 90°$) even more hydrophobic ($\beta^* > \beta$).

The conventional understanding is that hydrophilicity delays CHF because it promotes rewetting of dry patches that develop on the surface at high heat fluxes due to vigorous evaporation [16]. Conversely, hydrophobicity is thought to impair surface rewetting and thus reduce CHF. The best-known CHF correlation accounting for the effect of wettability is that of Kandlikar [17]:

$$q_{CHF} = \left[\frac{1+\cos \beta_r}{16}\right] \left[\frac{2}{\pi} + \frac{\pi}{4}(1 + \cos \beta_r)\cos \phi\right]^{\frac{1}{2}} \left[\rho_g^{\frac{1}{2}} h_{fg} \left[\sigma g(\rho_f - \rho_g)\right]^{\frac{1}{4}}\right] \tag{2}$$

where β_r is the receding contact angle, ρ_g is the gas phase density, ρ_f is the fluid phase density, h_{fg} is the enthalpy of vaporization, g is the gravitational constant and ϕ is the angular orientation of the heater, with $\phi = 0$ corresponding to the horizontal orientation. Thus, Eq. (2) implies that the only surface characteristic affecting CHF is contact angle.

Roughness is a measure of a surface's vertical (positive or negative) deviations from an ideal flat surface, and is typically described by the quantities R_a, the arithmetic average of the absolute value of surface feature heights, R_q, the root mean square (rms) of the surface feature heights, and R_z, the average distance of the five highest peaks to lowest five valleys. Roughness has historically been attributed to have large effects on the boiling heat transfer coefficient [18,19] and also CHF [20], presumably because higher values of roughness are usually associated with a larger number of micro-cavities that could become bubble nucleation sites. The CHF correlation of Ramilison *et al.* [20] is meant to account for the effects of surface roughness and also contact angle:

$$q_{CHF} = 0.0366[\pi - \beta_r]^{3.0} R_q^{0.125} \frac{\pi}{24} \left[\rho_g^{\frac{1}{2}} h_{fg} \left[\sigma g (\rho_f - \rho_g) \right]^{\frac{1}{4}} \right] \qquad (3)$$

In the context of this study, porosity refers to the presence of a porous layer on the surface; therefore it is described by the void fraction ε in the porous layer. Surface porosity could affect boiling heat transfer through a variety of hypothesized mechanisms, depending on the porous layer thickness, and number, size and interconnection of the pores. For example, micro-sized pores can increase the nucleation site density, by creating cavities to seed bubble formation [22]. Moreover, the interconnection of the porous structure allows for transport of liquid between nucleation sites. Therefore, rewetting of nucleation sites after bubble departure is enhanced, which can help delay CHF [22]. Surface rewetting is further promoted through capillary action induced by the porous structure [21]. On the other hand, if the matrix is hydrophobic, the fluid is repelled from the pores, which accelerates occurrence of CHF. The CHF correlation of Polezhaev and Kovalev [23] accounts for the effect of porosity and pore size:

$$q_{CHF} = 0.5\varepsilon^{2.28} h_{fg} \left[\frac{\sigma \rho_f \rho_g}{(\rho_f + \rho_g) R_{bg}} \right]^{\frac{1}{2}} \qquad (4)$$

where R_{bg} is the experimentally determined breakthrough radius, which can be considered approximately half the particle diameter for a porous layer composed of densely packed particles. Eq. 4 does not distinguish between porous layers that are hydrophilic or hydrophobic.

Equations 2, 3 and 4 each emphasize a different set of surface parameters, suggesting that there is no consensus on what surface parameter(s) actually govern CHF. This uncertainty stems in part from the fact that in all the experimental studies of surface effects on CHF conducted to date typically more than one surface parameter are changed simultaneously, thus making it hard to distinguish which parameter is important from which is not. Therefore, the election of one "important" surface parameter, be it roughness, wettability or porosity, in the correlations/models presented above is somewhat arbitrary. The objective of this study is to isolate experimentally the effects of surface porosity, roughness and wettability on CHF, so that a systematic and coherent understanding of the influence of the boiling surface on CHF phenomena can commence. This objective is accomplished through the use of carefully-engineered surfaces for which roughness, wettability and porosity can be changed precisely and independently.

Pool boiling tests with water at atmospheric pressure were conducted in the facility shown in Figure 1, consisting of an inner test bath and an outer isothermal bath. The isothermal bath was maintained at saturation (100°C) using a cartridge heater. The test sample design is shown in Figure 1: a thin (0.7 μm) Indium Tin Oxide (ITO) layer was deposited on a 0.25-mm-thick, 50.8x50.8 mm^2, nano-smooth, square sapphire substrate. The ITO was resistively heated by a DC power supply via silver electrodes. After thorough degassing, the heat flux was increased in small steps from zero to CHF. The temperature profile of the heater surface was obtained with an infrared camera at each heat flux. CHF was identified by a drastic temperature excursion on the infrared signal; additionally, CHF occurrence typically resulted in destruction of the sample.

Surface features were engineered on the uncoated side of the sapphire substrate. Surface roughness was controlled by implanting micro posts by photolithography [24], 15 μm tall, 20 μm in diameter, and spaced on a 500 μm hexagonal pitch. As we wished to isolate the effect of

roughness from that of wettability, the spacing of the posts was selected large enough to have a roughness factor close to unity ($r \sim 1$), so that the contact angle would not be affected, per Eq. 1. It was also verified that triple contact line pinning by the posts would not occur. Porosity was controlled by depositing 2.5-µm thick layers of silica nanoparticles of 50 nm diameter, using the layer-by-layer technique (LbL) [25]. The nanoparticles assemble in a loose packed fashion to around 50% of the total volume. Therefore, the pore size is of the order of the particle diameter. LbL enables creation of a very smooth porous layer, i.e. the roughness is a negligible 50 nm. Wettability was controlled by depositing thin, smooth, non-porous layers of hydrophilic (silica) or hydrophobic (fluorosilane) materials by Electron Beam Physical Vapor Deposition (EB-PVD) or Chemical Vapor Deposition (CVD), respectivey[26,27]. See Ref. 28 for more details about the fabrication procedures for all the samples tested in this study.

Nine combinations of surface roughness, wettability and porosity were analyzed, as shown in Table I. Surfaces were categorized as hydrophilic (static contact angle < 5°) or hydrophobic (static contact angle > 110°), smooth (R_z < 0.1 µm) or rough (R_z > 1 µm), porous (porosity ~50%) or non-porous (zero porosity). For each combination, at least three heaters were fabricated and tested, to ensure repeatability of the results.

The values for roughness, porosity and contact angle reported in Table I were measured by a surface profiler, spectroscopic ellipsometry and a goniometer, respectively. Representative images of the engineered surfaces are shown in Figure 2.

Table I. Measured values of surface parameters and CHF data.

Test #	Pattern	Fabrication	Roughness			Roughness factor, r	Porosity (vol%)	Contact angle (degrees)			CHF (kW/m^2)
			R_a (µm)	R_q (µm)	R_z (µm)			Static	Advancing	Receding	
1	Smooth Uncoated Heater (reference)	• No fabrication required	<0.01	0.01	<0.01	1	0	~75	82	48	920±77
2	Smooth Non-porous Hydrophilic	• Electron beam deposition of 20nm SiO$_2$ layer	<0.01	0.01	0.02	1	0	<5	~0	~0	1009±103
3	Smooth Non-porous Hydrophobic	• Electron beam deposition of 20nm SiO$_2$ layer • Chemical vapor deposition of fluorosilane	0.01	0.01	0.03	1	0	112	131	81	968±173
4	Smooth Porous Hydrophilic	• LbL deposition of 50nm diameter SiO$_2$ particles, fifty layers	0.14	0.18	0.78	~1	50	<5	~0	~0	1617±177
5	Smooth Porous Hydrophobic	• LbL deposition of 50nm diameter SiO$_2$ particles, fifty layers • Chemical vapor deposition of fluorosilane	0.12	0.15	0.72	~1	50	137	160	97	34±4
6	Rough Non-porous Hydrophilic	• Photolithography of 20µm diameter, 15µm tall posts; 0.5mm pitch • Electron beam deposition of 20nm SiO$_2$ layer	2.69	4.54	14.96	1.0044[*]	0	<5	~0	~0	1063±58
7	Rough Non-porous Hydrophobic	• Photolithography of 20µm diameter, 15µm tall posts; 0.5mm pitch • Electron beam deposition of 20nm SiO$_2$ layer • Chemical vapor deposition of fluorosilane	2.62	4.43	15.22	1.0044[*]	0	113	132	86	1067±163
8	Rough Porous Hydrophilic	• Photolithography of 20µm diameter, 15µm tall posts; 0.5mm pitch • LbL deposition of 50nm diameter SiO$_2$ particles, fifty layers	2.22	3.95	14.08	1.0044[*]	50	<5	~0	~0	1591±111
9	Rough Porous Hydrophobic	• Photolithography of 20µm diameter, 15µm tall posts; 0.5mm pitch • LbL deposition of 50nm diameter SiO$_2$ particles, fifty layers • Chemical vapor deposition of fluorosilane	2.05	3.73	13.25	1.0044[*]	50	140	149	104	20-40

[*] Estimated as $r = 1 + 2\pi DH/(S^2\sqrt{3})$, where D, H and S are the diameter, height and spacing of the posts, respectively.

The rightmost column in Table I reports the CHF data, from which it is possible to draw several observations. First, wettability alone did not appreciably affect CHF: the uncoated (test 1), smooth non-porous hydrophilic (test 2) and smooth non-porous hydrophobic surfaces (test 3), in spite of a contact angle difference of more than 100°, had similar values of CHF. (The contact angles were measured again after the boiling tests, to confirm they had not changed.) These surprising results suggest that wettability alone does not govern CHF, which conflicts with the assumption in Eq. 2.

Second, porosity had a dramatic effect on CHF: smooth porous hydrophilic surfaces (test 4) realized CHF enhancements of up to 60% with respect to the reference heater and had the highest absolute CHF values of any feature tested. Conversely, hydrophobic porous surfaces (test 5) exhibited a CHF *reduction* of up to 97%, i.e. essentially the heater transitioned immediately to film boiling. These results suggest that the sign and magnitude of the effect of porosity on CHF depend on the wettability of the porous layer, a dependence that is not captured by Eq. 4. We hypothesize that the effect of porosity on CHF is through capillary wicking within the pores: if the pores are hydrophilic, water is pulled to the surface, which delays CHF. Vice versa, if the pores are hydrophobic, water is repelled from the pores and CHF is accelerated.

Third, roughness (R_a, R_q, R_z) per se, although varied over two orders of magnitude, did not affect CHF at all on the engineered surfaces interrogated here, regardless of any other surface parameters present. All the rough heaters tested (tests 6, 7, 8 and 9) behaved similarly to their smooth counterparts (tests 2, 3, 4 and 5, respectively). As the roughness results were unexpected, additional tests were conducted with two more values of post height and two more values of post spacing, for the hydrophilic surface. The results are shown in Table II, where the CHF value for test 6 is reported again for convenience of comparison. It can be seen that indeed there is no meaningful effect of post height on CHF, at a given post spacing. However, when the post spacing is reduced enough to yield a roughness factor (r) significantly larger than unity, the CHF increases by a large amount, i.e. ~60%. CHF experiments with surfaces featuring tightly-spaced posts were conducted also by Chu et al.[10,29]. In their papers, Kandlikar's model (Eq. 2) was modified to account for the effect of the posts on the surface force per unit length

maintaining the position of the contact line underneath a bubble; they suggested that, for a given fluid, CHF should scale with receding contact angle and roughness ratio as follows:

$$q_{CHF} \propto \left[\frac{1+\cos\beta_r}{16}\right]\left[\frac{2(1+\alpha)}{\pi(1+\cos\beta_r)} + \frac{\pi}{4}(1+\cos\beta_r)\cos\phi\right]^{\frac{1}{2}} \qquad (5)$$

where $\alpha = r\cos\beta_r$. The CHF values predicted from Eq. 5 (normalized to the value from test 6) are shown in the right-most column of Table II. The trend predicted by the equation is correct: i.e., no CHF enhancement for tests 10, 11 and 12, and some CHF enhancement for test 13. However, the magnitude of the enhancement predicted for test 13 is significantly lower than the measured value.

Finally, it is interesting to note that CHF increased by a similar magnitude (about 60%) for porous hydrophilic surfaces (tests 4 and 8) and surfaces with tightly-spaced posts (test 13) with respect to the smooth non-porous hydrophilic surface (test 6). Using Eq. 5 for tests 4 and 8, we estimate that the value of the roughness ratio required to obtain a 60% enhancement is ~12. Such high value of r is plausible only if one accounts for the internal surface area of the pores, which is consistent with the hypothesis that capillary wicking in the pores is the mechanism responsible for CHF enhancement.

Table II. Effect of post height and spacing on CHF of non-porous, hydrophilic surfaces (β_r<5° for all surfaces). (each test was repeated three times)

Test #	Surface	Roughness (µm) $R_z/R_a/R_q$	Roughness factor[*], r	CHF (kW/m²)	CHF/CHF_ref. Measured	From Eq. 5
6	Posts 15 µm height, 500 µm spacing	15.0/2.7/4.5	1.0044	1063±58	1	1
10	Posts 10 µm height, 500 µm spacing	10.0/0.8/2.0	1.0029	957±55	~1	~1
11	Posts 5 µm height, 500 µm spacing	5.0/0.4/1.0	1.0015	940±113	~1	~1
12	Posts 15 µm height, 100 µm spacing	15.0/4.8/6.0	1.1088	975±58	~1	~1
13	Posts 15 µm height, 50 µm spacing	15.0/7.2/7.3	1.4353	1636±112	~1.6	1.03

[*] $r = 1 + 2\pi DH/(S^2\sqrt{3})$, where D, H and S are the diameter, height and spacing of the posts, respectively

It is important to recognize the difference between the engineered surfaces analyzed in this study and typical surfaces encountered in heat transfer application. Here, surface features were purposely defined such that roughness-type features did not exhibit any behavior of porosity-type features (except for test 13). In reality, the features of a heat transfer surface often result in a compound behavior representative of both roughness and porosity. As such, our analysis does not invalidate the semi-empirical correlations (Eqs. 2-4), which remain valid within the limits of their own respective databases, but rather suggests that the set of correlating parameters considered in the past was not optimal and likely incomplete. Our data show that the traditional measures of roughness (R_a, R_q and R_z) are not appropriate correlating parameters for CHF. A suitable set of correlating parameters for new CHF models/correlations for engineered surfaces can be derived from dimensional analysis: briefly, we introduce a dimensionless boiling number $Bo_{CHF} \equiv \frac{q_{CHF}}{\rho_g^{\frac{1}{2}} h_{fg} [\sigma g(\rho_f - \rho_g)]^{\frac{1}{4}}}$, which captures the established dependence of CHF on the fluid properties and gravity [30]. If we assume that the effects of surface features are driven by capillary wicking, then we expect the governing variables to be: void fraction (ε), effective pore diameter (D_p), effective pore length (L), intrinsic contact angle (β), surface tension (σ), fluid viscosity (μ_f), and fluid density (ρ_f). The above set of variables would apply to actual porous layers as well as any other open surface structure (e.g., tightly spaced posts) for which one can define a ratio of open to solid volume (void fraction), and effective diameter and length of the open paths for liquid wicking. The governing π-groups are ε and β themselves, the ratio D_p/L, and the pore Reynolds number $Re_p \equiv \rho_f \sigma D_p / \mu_f^2$. Therefore, the general functional form of a CHF correlation/model accounting for surface effects should be as follows:

$$Bo_{CHF} = f(Re_p, \frac{D_p}{L}, \varepsilon, \beta) \qquad (6)$$

Having determined the key role played by porosity, future work should focus on elucidating the effects of pore size, pore volume and porous layer thickness on CHF, so that the dependences expressed by Eq. 6 can be quantified, and optimized surfaces be created.

References

[1] N. Todreas and M. Kazimi, Nuclear Systems I: Thermal Hydraulic Fundamentals, New York: Taylor and Francis, 1993.

[2] S. S. Kutateladze, 1952, "Heat Transfer in Condensation and Boiling", AEC-TR-3770.

[3] N. Zuber, 1959, "Hydrodynamic Aspects of Boiling Heat Transfer", AECU-4439.

[4] E. Forrest, E. Williamson, J. Buongiorno, L. W. Hu, M. Rubner, R. Cohen, Int. J. Heat Mass Transfer, 53, 58–67 (2010).

[5] H. Kim, J. Kim, M. Kim, Nuclear Engineering and Technology, Vol. 38, No. 1, 61-68 (2006).

[6] P. Berenson, On Transition Boiling Heat Transfer from a Horizontal Surface, PhD Thesis, MIT, 1960.

[7] J. Chang and S. You, Int. J. Heat Mass Transfer, vol. 40, no. 18, pp. 4449-4460 (1997).

[8] R. Chen, M. Lu, V. Srinivassan, Z. Wang, H. Cho, and A. Majumdar, Nano Letters, no. 9, pp. 548-553 (2009).

[9] S. You and J. O'Connor, J. Heat Transfer, no. 117, pp. 687-692 (1995).

[10] K.-H. Chu, R. Enright, E. N. Wang, Applied Physics Letters, 100(24), p. 241603-00 (2012).

[11] V. K. Dhir, Annual Review Fluid Mechanics, 30, pp.365-401 (1998).

[12] H. Honda, H. Takamastu, J.J. Wei, ASME J. Heat Transfer, Vol. 124, 383-390 (2002).

[13] Y. Takata, S. Hidaka, M. Masuda, T. Ito, Int. J. Energy Res., 27, 111-119 (2003).

[14] S. Malla, M. Amaya, S. M. You, 8th Int. Conf. Multiphase Flow (ICMF 2013), Paper 128, Jeju, Korea, May 26-31 (2013).

[15] R. N. Wenzel, J. Physical Colloid Chemistry, 53, 9, 1466 (1949).

[16] T. G. Theofanous and T. N. Dinh, Multiphase Science and Technology, Vol. 18, No. 3, pp. 251-276 (2006).

[17] S. Kandlikar, J. Heat Transfer, Vol. 123, 1071-1079 (2001).

[18] P. Berenson, Int. J. Heat Mass Transfer, no. 5, pp. 985-999 (1962).

[19] I. L. Pioro, W. Rohsenow and S. S. Doerffer, Int. J. Heat Mass Transfer, Vol. 47, No. 23, pp. 5033-5044 (2004).

[20] J. Ramilison, P. Sadasivan and J. Lienhard, J. Heat Transfer, vol. 114, pp. 297-290 (1992).

[21] S. Liter, Int. J. Heat Mass Transfer, no. 22, pp. 4287-4311 (2001).

[22] M. Toprak, S. Li, B. Palm and M. Muhammed, J. Heat Transfer, vol. 131, no. 10, 101010 (2009).

[23] Y. Polezhaev and S. Kovalev, Thermal Engineering, vol. 37, no. 12, pp. 617-620 (1990).

[24] Micro Chem, "SU-8 2000 Permanent Epoxy Negative Photoresist Processing Guidlines, Version 4," Micro Chem, Newton, MA.

[25] D. Lee, Z. Gemici, M. Rubner, and R. Cohen, Langmuir, no. 23, pp. 8833-8837 (2007).

[26] U. Heisig, S. Schiller and S. Panzer, Electron bean technology, Wiley, 1995.

[27] D. Mattox, Handbook of Physical Vapor Deposition (PVD) Processing, Noyes Publications, 1998.

[28] H. O'Hanley, Separate Effects of Surface Roughness, Wettability and Porosity on Boiling Heat Transfer and Critical Heat Flux and Optimization of Boiling Surfaces, MIT Masters Thesis, 2012.

[29] K.-H. Chu, R. Enright, S. Joung, C. E. Buie, E. N. Wang, Applied Physics Letters, 102, 151602 (2013).

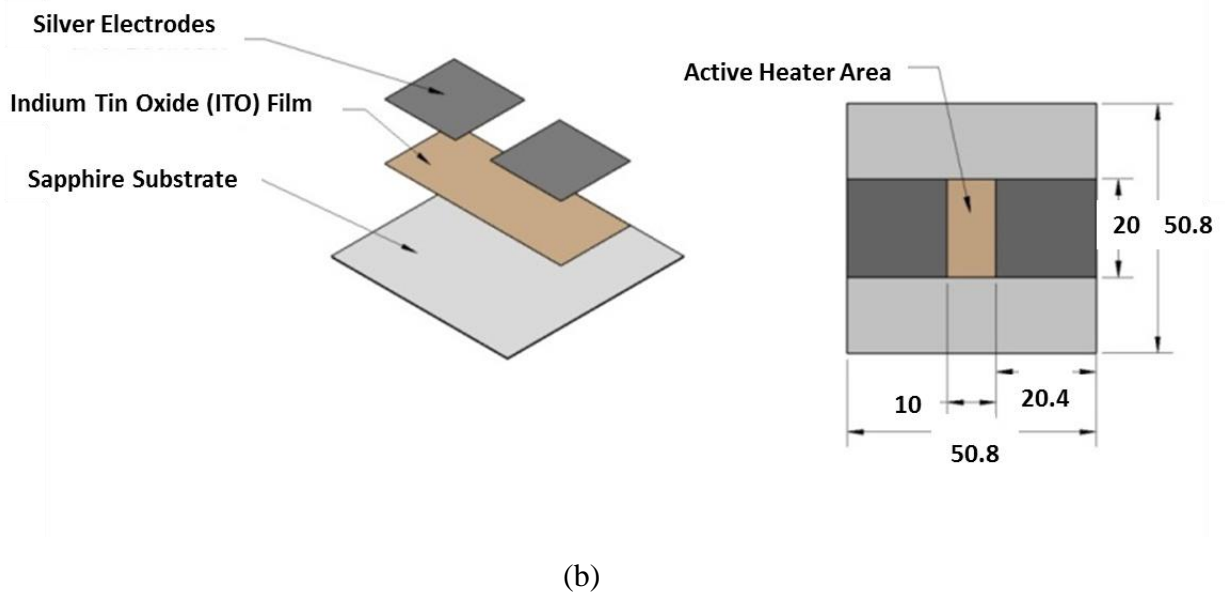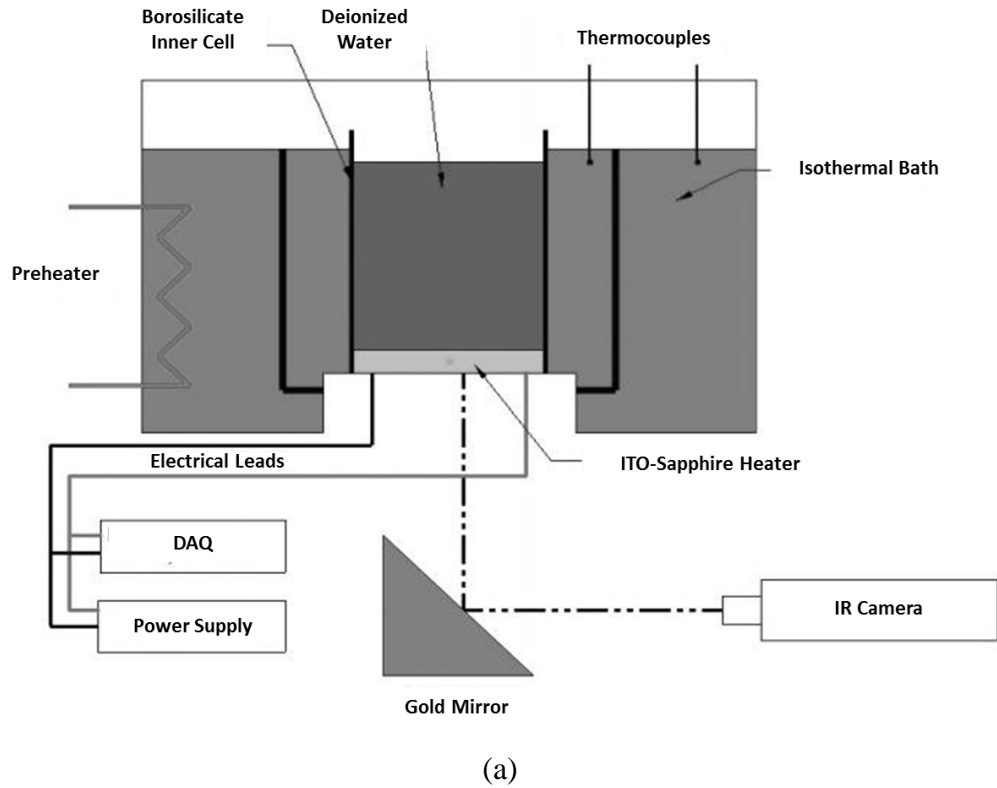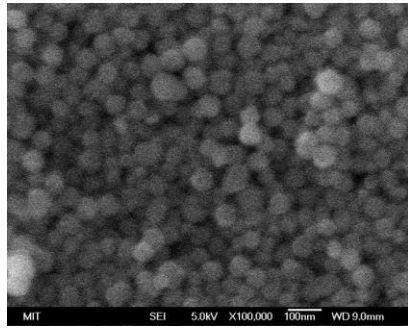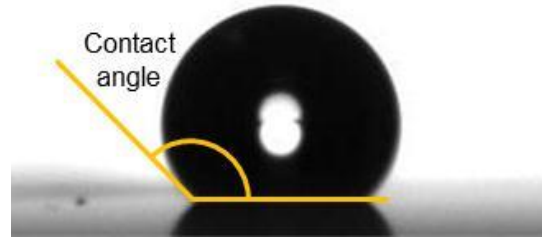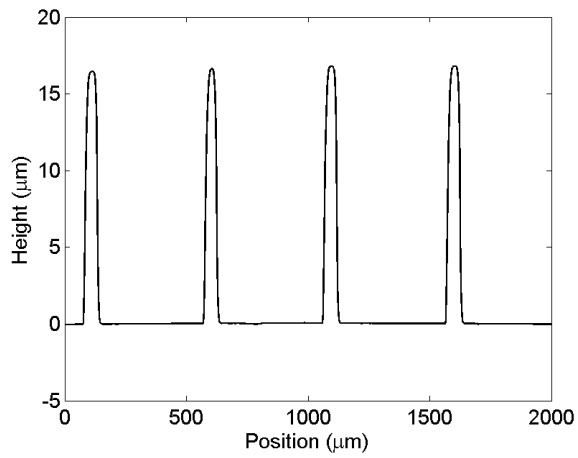[30] S. Kandlikar, J. Heat Transfer, Vol. 126, pp. 8-16 (2004).

(a)

(b)

FIG. 1. (a) Pool boiling facility and (b) design of ITO-sapphire heater with relevant dimensions (in mm).
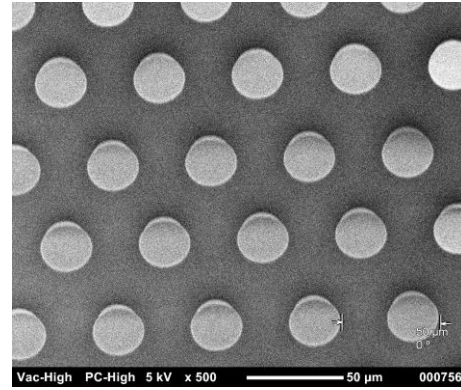
(a)

(b)

(c)

(d)

FIG. 2. (a) Scanning electron microscope (SEM) image of smooth porous hydrophilic heater at 100,000x. (b) Contact angle of water droplet on the smooth non-porous hydrophobic surface. (c) Measured profile of posts. (d) SEM image of tightly-spaced posts.